

RESEARCH

Open Access



# An improved bacterial mRNA enrichment strategy in dual RNA sequencing to unveil the dynamics of plant-bacterial interactions

Jayabalan Shilpha<sup>1†</sup>, Junesung Lee<sup>1†</sup>, Ji-Su Kwon<sup>1†</sup>, Hyun-Ah Lee<sup>2</sup>, Jae-Young Nam<sup>1</sup>, Hakgi Jang<sup>1</sup> and Won-Hee Kang<sup>1\*</sup>

## Abstract

**Background** Dual RNA sequencing is a powerful tool that enables a comprehensive understanding of the molecular dynamics underlying plant-microbe interactions. RNA sequencing (RNA-seq) poses technical hurdles in the transcriptional analysis of plant-bacterial interactions, especially in bacterial transcriptomics, owing to the presence of abundant ribosomal RNA (rRNA), which potentially limits the coverage of essential transcripts. Therefore, to achieve cost-effective and comprehensive sequencing of the bacterial transcriptome, it is imperative to devise efficient methods for eliminating rRNA and enhancing the proportion of bacterial mRNA. In this study, we modified a strand-specific dual RNA-seq method with the goal of enriching the proportion of bacterial mRNA in the bacteria-infected plant samples. The enriched method involved the sequential separation of plant mRNA by poly A selection and rRNA removal for bacterial mRNA enrichment followed by strand specific RNA-seq library preparation steps. We assessed the efficiency of the enriched method in comparison to the conventional method by employing various plant-bacterial interactions, including both host and non-host resistance interactions with pathogenic bacteria, as well as an interaction with a beneficial rhizosphere associated bacteria using pepper and tomato plants respectively.

**Results** In all cases of plant-bacterial interactions examined, an increase in mapping efficiency was observed with the enriched method although it produced a lower read count. Especially in the compatible interaction with *Xanthomonas campestris* pv. *Vesicatoria* race 3 (Xcv3), the enriched method enhanced the mapping ratio of Xcv3-infected pepper samples to its own genome (15.09%; 1.45-fold increase) and the CDS (8.92%; 1.49-fold increase). The enriched method consistently displayed a greater number of differentially expressed genes (DEGs) than the conventional RNA-seq method at all fold change threshold levels investigated, notably during the early stages of Xcv3 infection in peppers. The Gene Ontology (GO) enrichment analysis revealed that the DEGs were predominantly enriched in proteolysis, kinase, serine type endopeptidase and heme binding activities.

<sup>†</sup>Jayabalan Shilpha, Junesung Lee and Ji-Su Kwon contributed equally to this work.

\*Correspondence:  
Won-Hee Kang  
whkang@gnu.ac.kr

Full list of author information is available at the end of the article



© The Author(s) 2024. **Open Access** This article is licensed under a Creative Commons Attribution 4.0 International License, which permits use, sharing, adaptation, distribution and reproduction in any medium or format, as long as you give appropriate credit to the original author(s) and the source, provide a link to the Creative Commons licence, and indicate if changes were made. The images or other third party material in this article are included in the article's Creative Commons licence, unless indicated otherwise in a credit line to the material. If material is not included in the article's Creative Commons licence and your intended use is not permitted by statutory regulation or exceeds the permitted use, you will need to obtain permission directly from the copyright holder. To view a copy of this licence, visit <http://creativecommons.org/licenses/by/4.0/>. The Creative Commons Public Domain Dedication waiver (<http://creativecommons.org/publicdomain/zero/1.0/>) applies to the data made available in this article, unless otherwise stated in a credit line to the data.

**Conclusion** The enriched method demonstrated in this study will serve as a suitable alternative to the existing RNA-seq method to enrich bacterial mRNA and provide novel insights into the intricate transcriptomic alterations within the plant-bacterial interplay.

**Keywords** *Capsicum annuum*, Dual RNA-seq, Gene ontology, Plant-bacterial interactions, Poly A selection, rRNA depletion

## Background

Functional genomics and the ease of access to next-generation sequencing (NGS) techniques have brought about a profound revolution in the field of gene expression research [1]. Over the past decade, there has been a growing preference for high throughput RNA sequencing (RNA-seq) technology in transcriptome research over conventional microarray technology [2, 3]. This preference is driven by its enhanced ability to precisely quantify gene expression levels, offering greater sensitivity and specificity in both eukaryotic and prokaryotic organisms [4–8]. Besides the potential for achieving complete genome coverage, RNA-seq offers various advantages over microarray and tag-based methods. These include an unlimited dynamic range, reduced bias, independence from annotations, and the absence of issues related to probe design or cross-hybridization [9, 10]. RNA-seq can distinguish between different mRNA isoforms and non-coding RNAs (ncRNAs), as well as detect splice junctions and precisely locate transcript boundaries [11–14]. In spite of these advantages, RNA-seq for the transcriptional analysis of plant-microbe interactions remains technically challenging, particularly with the microbial transcriptomics. Employing the transcriptomic approach in bacterial cells presents a significant hurdle owing to the considerable abundance of ribosomal RNA (rRNAs), which make up more than 95% of the entire cellular RNA content [15]. As a result, the effective coverage of valuable transcripts is significantly diminished. Hence, achieving cost-effective and comprehensive sequencing of the bacterial transcriptome necessitates the formulation of effective methods for depleting the abundant bacterial rRNA molecules viz., 5 S, 16 S, and 23 S rRNA [16].

Currently, three primary approaches are employed for rRNA depletion. The first uses oligonucleotide hybridization, followed by magnetic bead separation [17]. The second employs complementary oligonucleotide annealing and enzymatic digestion of duplex hybrids using specific nucleases [18]. The third restricts cDNA synthesis to non-rRNA templates through a specialized primer mixture during cDNA synthesis, excluding rRNA matches [19]. Numerous commercially available kits have been used for eliminating bacterial rRNA from total RNA samples. These encompass the MICROBExpress bacterial mRNA enrichment kit from Thermo Fisher Scientific, the MICROBEnrich™ kit, from Thermo Fisher Scientific and Ambion, the RiboMinus transcriptome isolation kit

for bacteria from Thermo Fisher Scientific, NEBNext bacteria rRNA depletion kit from New England Biolabs, mRNA-ONLY prokaryotic mRNA isolation Kit from Epicentre Biotechnologies, Terminator™ kit from Lucigen, Ribo-Zero rRNA depletion kit from Illumina and Epicentre and riboPOOLS from siTOOLS [20, 21]. Among them, the mRNA-ONLY and Terminator kits operate based on the concept of utilizing 5′-monophosphate-dependent exonuclease to break down the processed RNA molecules with 5′-phosphorylation, like rRNAs. However, this approach has exhibited lower effectiveness compared to alternative rRNA depletion methods, resulting in only a moderate enhancement (1.9 to 5.7-fold) of bacterial mRNA enrichment, with fewer than 25% of aligned sequencing reads corresponding to transcripts other than rRNA [22]. The MICROBEnrich™ kit utilizes an innovative magnetic bead capture hybridization technique to effectively remove mammalian RNA (including human, mouse, or rat RNA) from intricate mixtures of mammalian host-bacterial RNA [23, 24]. This method eliminates over 90% of mammalian RNA by concomitantly eliminating polyadenylated mRNAs along with 18 S rRNA and 28 S rRNA. Nevertheless, MICROBEnrich does not eliminate small RNAs like 5 S rRNA and tRNA from the enriched bacterial RNA pool. Therefore, it necessitates the utilization of additional kits to eliminate small RNAs before initiating the MICROBEnrich procedure. Similarly, the MICROBExpress and RiboMinus kits target oligonucleotides corresponding to 16 S and 23 S rRNA but do not eliminate 5 S rRNA. In contrast, Ribo-Zero kit captures 5 S rRNA in addition to 16 S and 23 S rRNA by magnetic beads. Unlike MICROBEnrich, Ribo-Zero kits do not simultaneously eliminate poly A mRNA. Instead, they selectively deplete rRNA from total RNA samples, allowing for a more comprehensive examination of the non-rRNA portion of the transcriptome. Many studies have demonstrated the effectiveness of the Ribo-Zero kit in eliminating rRNA preceding the RNA-seq library construction [16, 20, 23–25]. Thus, employing Ribo zero kits along with poly A mRNA selection represents an optimal tactic to improve dual RNA sequencing of host-bacterial samples, as demonstrated in this study.

Comprehending the intricate interaction between infecting bacteria and their eukaryotic host is crucial for unraveling the pathogenesis and advancement of diseases as well as their persistence within host cells. Through the concurrent capture of active genes from both the

bacteria and the host, dual RNA-seq offers a comprehensive overview of the molecular dynamics involved in bacterial infection processes and the corresponding host responses. However, the profiling of *in planta* bacterial transcriptomes in dual RNA-seq presents several challenges. For instance, bacterial RNAs might comprise less than 1% of the total RNA content, whereas plant rRNA can make up as much as 98% of the total RNA within an infected cell. Particularly, acquiring sufficient bacterial RNA during early stages of infection remains a notable challenge [26]. Compared to standard transcriptomic investigations, dual RNA sequencing introduces technical hurdles arising from the varying proportion of reads originating from the less abundant (bacterial) transcripts in contrast to the more abundant (plant) transcripts, along with the substantial difference in total RNA content where the host significantly outnumbers the bacterial counterpart [15]. Therefore, along with the removal of rRNA, it is imperative to implement mRNA enrichment approaches to guarantee cost-effective sequencing of an ample amount of non-rRNA sequences [16]. Prokaryotic mRNAs are relatively less stable and lack a 3' polyadenylated tail, hindering hybridization capture, cDNA synthesis, and poly (T) oligomer amplification [27]. Conversely, eukaryotic mRNAs are stable, contain elongated poly (A) tails, and can be enriched using oligo (dT) primers, effectively isolating them from rRNA molecules for sequencing library construction. PCR amplification plays a crucial role in well-known RNA-seq library construction methods such as TruSeq, in enhancing the concentration of cDNA prior to sequencing [28]. Nonetheless, there remains an uncertainty regarding the impact of PCR on the mapping ratio to the genome and coding sequences (CDS), as well as the extent to which PCR amplification introduces noises, potentially diminishing the accuracy of transcript quantification.

Several pathogenic bacteria affect a wide range of crops worldwide, causing considerable damage to crop output and consequently significant financial losses. Bacterial leaf spot is one of the common and devastating diseases in pepper (*Capsicum annuum* L.) and tomato (*Solanum lycopersicum* L.) caused by *Xanthomonas campestris* pv. *vesicatoria* (Xcv) leading to significant defoliation, decreased plant vitality and substantial reductions in crop yield [29, 30]. Generally, host-pathogen interactions can be categorized into two primary categories: (1) a compatible interaction, which lead to a successful infection and subsequent disease (2) an incompatible interaction, where the pathogen is successfully defeated by the plant's defense mechanisms. In case of an incompatible interaction, as a resistance measure, plants trigger a hypersensitive response (HR), which is a cellular death response that occurs at the entry point of the pathogen, effectively halting the further advancement

of the pathogen [31]. The HR responses caused by *Xanthomonas axonopodis* pv. *glycines* (Xag) is an example for an incompatible non-host interaction in pepper plants [32]. On the other hand there are several rhizosphere associated bacteria which mostly exert neutral effect or positive effect on the growth and wellbeing of their host plants through complex interactions [33]. *Flavobacterium dauae*, is one such bacterial strain isolated from the rhizosphere soil of tomato [34]. The understanding of various plant-bacterial interactions will aid in the development of innovative strategies for managing bacterial diseases. Thus, the documentation of transcriptomic profiles of both the host and bacteria at various time points following infection could facilitate the examination of the molecular changes driving host responses and bacterial adaptability. In the present investigation, we have devised a high throughput dual RNA sequencing method involving mRNA enrichment strategies such as rRNA depletion combined with poly A enrichment using Dynabeads, to investigate the molecular dynamics involved in host-bacterial interactions using tomato and pepper plants. Moreover, the effect of PCR cycles on the mapping ratio of plant-bacterial samples to the genome and CDS of bacteria has been examined.

## Materials and methods

### Plant materials and bacterial inoculation

To assess the host-bacterial interactions, the tomato cultivar 'Heinz' was inoculated with *Flavobacterium dauae*, a beneficial rhizosphere associated bacteria. Hot pepper cultivars, 'ECW30R', and 'Bukang' were inoculated with *Xanthomonas campestris* pv. *vesicatoria* race 3 (Xcv3) showing host resistant response and *Xanthomonas axonopodis* pv. *glycines* 8ra (Xag8ra) showing non-host resistant response. The *F. dauae* was cultured in Trypticase Soy Agar (TSA) media at 30°C for 2 days and subsequently diluted to a concentration of 10<sup>9</sup> CFU/mL in Hoagland solution (Sigma-Aldrich, St. Louis, CA, USA). The *F. dauae* suspension was inoculated into 3 days-post-germination-stage of tomato seedlings. Then, *F. dauae* inoculated plants were grown in a growth chamber at 28°C and 16-h light / 8-h dark photoperiod, and inoculated seedlings were harvested at 48 h post inoculation (hpi). For the preparation of Xcv3 and Xag8ra inocula, we followed the methods as described previously [31, 35]. Xcv3 and Xag8ra were cultured in Luria-Bertani (LB) media containing rifampicin (50 mg/L) for 2 days and then were suspended in 10 mM MgCl<sub>2</sub> and diluted to a final concentration of 10<sup>8</sup> CFU/mL. Subsequently, Xcv3 and Xag8ra suspensions were infiltrated into the leaves of 6 true-leaf-stage of 'ECW30R' and 'Bukang', respectively. The leaves of Xcv3 inoculated pepper plants were harvested at 12, 24, and 48 hpi, whereas Xag8ra inoculated plants were sampled at 48 hpi. All bacterial inoculation

was performed in at least three independent experiments with 12–16 plants for each experiment. The pathogen control for Xcv3 was prepared using a suspension in 10 mM MgCl<sub>2</sub> at a concentration of 10<sup>8</sup> CFU/mL.

#### RNA extraction and RNA-seq library construction

Total RNA was extracted from the leaves of pepper and roots of tomato seedlings (100 mg) using Trizol reagent (Invitrogen, Carlsbad, CA, USA) following the manufacturer's instructions. RNA-seq libraries were prepared from the five microgram of RNA using TruSeq kit (Illumina, San Diego, CA, USA; hereafter conventional method) and modified strand-specific method (hereafter enriched method). For the conventional method, we performed the construction of RNA-seq libraries using TruSeq preparation kit with ribo depletion following the manufacturer's recommendations. For the enriched method, we used a modified strand-specific library construction method [36–38]. To isolate the poly A RNA, the RNA samples were treated with Dynabeads™ oligo(dT)<sub>25</sub> (Invitrogen, Carlsbad, CA, USA) and collected separately. In the conventional method, 1X volume (15 µL) of Dynabeads is used while for the enriched method, 3.3X (50 µL) of Dynabeads are employed, denoted as B1X and B3.3X respectively. The 1X volume of Dynabeads was also tested for the enriched method as the reference. For the mock controls (*C. annuum* and Xcv3), the conventional RNA-seq method was applied with 1X concentration of Dynabeads being used for *C. annuum* and no Dynabeads added for Xcv3 (Table 1). The remaining RNA samples without Dynabeads™ oligo(dT)<sub>25</sub> were subjected to ribo depletion by Ribo-Zero Plant Kit (Illumina, San Diego, CA, USA) to remove rRNAs from both plant and bacteria in the proportion of 95:5 according to host vs. bacteria ratio in infected samples. Subsequently, the rRNA removed and poly A removed RNA samples were pooled together and progressed to cDNA synthesis. The sequential steps for library construction were carried out following the strand-specific library method as previously described [36–38]. Further, to optimize the enriched method 10, 12, 15, or 20 cycles of PCR enrichment were performed to prepare the libraries. The quality and size (approximately 200–400 bp in size) of all libraries were evaluated with Agilent 2100 Bioanalyzer (Agilent Technologies, Inc., Santa Clara, CA, USA).

#### Sequencing and data processing

The libraries were sequenced using a 101-nt, paired-end module on a HiSeq 2000 platform (Illumina, San Diego, CA, USA). The low quality reads and adapter sequences were filtered and trimmed using Cutadapt [39] and Trimmomatic [40]. The rRNA filtering was performed using SortMeRNA (version 2.1b) and the silva database [41, 42]. The processed clean reads were aligned to reference

genome and gene model of each sample including *F. dauae* TCH3–2 (GCF\_004151275.1 ASM415127v1), Xcv3 (GCF\_000009165.1 ASM916v1), and Xag8ra (GCF\_001854145.2 ASM185414v2) using Hisat v2-2.1.0 software with default values [43]. Hierarchical clustering of transcriptomes for sample validation was performed using the hclust function in R. Raw read counts were normalized using FPKM methods [44]. Differential expressed genes (DEGs) were identified from comparison between Xcv3 treated samples and the pathogen mock control using the DESeq2 [45] package (FDR < 0.05). The database construction for Gene Ontology (GO) enrichment analysis was performed using BLAST2GO [46] for *Xanthomonas* gene functional annotation. Based on the constructed GO database, GO enrichment analysis was performed using Goseq [47]. The GO enrichment results were visualized using ggplot2 R package [48].

#### Real-time qRT-PCR measurements

Quantitative reverse transcription PCR (qRT-PCR) assays were conducted with the same total RNA samples that were used for DEG profiling of Xcv3. The real-time qRT-PCR was performed using Rotor Gene Q system (QIAGEN, Hilden, Germany) and PCR primers were designed with Primer3 plus software and the primers used for validation is listed in Table S1. Reverse transcription (RT) of 80 ng total RNA was carried out in a total volume of 20 µl with a Superscript® IV Reverse Transcriptase (Invitrogen, Waltham, MA, USA) using random hexamers. Cycling parameters were initial denaturation at 95°C for 2 min, then 50 cycles of 95°C for 20 s, 20 s at primer specific annealing temperatures, and 72°C for 20 s, followed by a cDNA dissociation program from 72 to 95°C. Each 20 µl reaction mixture contained 8 µl of diluted cDNA (1:5), 2 µl of each primer (10 µM) and 10 µl of 2X QuantiNova™ SYBR Green master mix (QIAGEN, Hilden, Germany). Serial dilutions of the pooled cDNA samples were used to generate standard curves to acquire the amplification efficiencies of PCR reactions. A bacteria specific gene encoding *lepA* was selected as the reference gene [49]. We normalized the expression of the target gene using housekeeping genes and also carried out normalization based on Xcv3-12 hpi cDNA samples to measure the relative expression value. Our preliminary evaluation indicated that expression of *lepA* displays little variation across all samples tested. All real-time qRT-PCR assays were carried out in three independent parallel experiments.

## Results

### Experimental design for the enrichment of bacterial mRNA in plant-bacterial sample

In the present study, in order to perform the enrichment of bacterial RNAs within plant samples infected by

**Table 1** Statistical summary and comparative read mapping of RNA-seq data used in the study

| Plant                           | Bacteria            | Type of pant-bacterial interaction | Method       | Time point (hpi) | Modification <sup>a</sup> | Clean reads <sup>b</sup> | Plant                      |                                      | Bacteria                   |                                      | Mapped CDS ratio <sup>f</sup> (%) |       |
|---------------------------------|---------------------|------------------------------------|--------------|------------------|---------------------------|--------------------------|----------------------------|--------------------------------------|----------------------------|--------------------------------------|-----------------------------------|-------|
|                                 |                     |                                    |              |                  |                           |                          | Mapped genome <sup>c</sup> | Mapped genome ratio <sup>d</sup> (%) | Mapped genome <sup>c</sup> | Mapped genome ratio <sup>d</sup> (%) |                                   |       |
| <i>S. lycopersicum</i>          | <i>F. drouae</i>    | Positive                           | Conventional | 48               | B1X/C10                   | 119,836,355              | 114,930,404                | 95.91                                | 1,434,056                  | 1.2                                  | 183,600                           | 0.15  |
|                                 |                     |                                    | Enriched     | 48               | B1X/C10                   | 12,299,298               | 11,505,248                 | 92.3                                 | 127,753                    | 1.1                                  | 70,554                            | 0.57  |
|                                 |                     |                                    |              |                  | B3.3X/C10                 | 18,368,732               | 17,565,053                 | 95.41                                | 353,341                    | 1.94                                 | 182,212                           | 0.99  |
| <i>C. annuum</i>                | Xag8ra              | Incompatible, non-host resistance  |              |                  | B3.3X/C15                 | 16,216,836               | 15,577,275                 | 94.98                                | 273,359                    | 1.8                                  | 149,081                           | 0.9   |
|                                 |                     |                                    |              |                  | B3.3X/C20                 | 13,658,775               | 13,095,302                 | 95.47                                | 205,142                    | 1.55                                 | 109,220                           | 0.8   |
|                                 |                     |                                    |              |                  | B3.3X/C15                 | 23,631,656               | 21,521,157                 | 91.07                                | 212,168                    | 0.90                                 | 144,087                           | 0.61  |
|                                 |                     |                                    |              |                  | B3.3X/C20                 | 146,198,300              | 131,961,491                | 90.59                                | 1,475,467                  | 0.94                                 | 1,007,895                         | 0.64  |
|                                 |                     |                                    |              |                  | B3.3X/C10                 | 26,886,048               | 24,293,063                 | 90.47                                | 496,519                    | 1.81                                 | 332,082                           | 1.21  |
| <i>C. annuum</i>                | Xcv3                | Incompatible, host resistance      |              |                  | B3.3X/C15                 | 23,797,803               | 21,503,984                 | 90.31                                | 507,576                    | 2.16                                 | 347,292                           | 1.48  |
|                                 |                     |                                    |              |                  | B3.3X/C20                 | 45,286,688               | 40,699,396                 | 89.82                                | 1,143,759                  | 2.55                                 | 846,593                           | 1.89  |
|                                 |                     |                                    |              |                  | B3.3X/C12                 | 26,275,757               | 22,468,782                 | 85.6                                 | 194,644                    | 0.74                                 | 103,713                           | 0.39  |
| <i>C. annuum</i>                | Xcv3                | Incompatible, host resistance      |              |                  | B3.3X/C12                 | 24,281,467               | 21,360,839                 | 88.03                                | 509,365                    | 2.12                                 | 317,319                           | 1.32  |
|                                 |                     |                                    |              |                  | B3.3X/C12                 | 24,790,157               | 18,854,536                 | 76.17                                | 3,781,607                  | 15.09                                | 2,249,053                         | 8.92  |
|                                 |                     |                                    |              |                  | B1X/C10                   | 30,157,170               | 27,458,323                 | 91.03                                | 159,407                    | 0.53                                 | 99,825                            | 0.33  |
|                                 | Xcv3 (Mock control) |                                    | Conventional | 24               | B1X/C10                   | 34,311,587               | 31,031,802                 | 90.44                                | 494,298                    | 1.44                                 | 290,749                           | 0.85  |
|                                 |                     |                                    | Conventional | 48               | B1X/C10                   | 30,267,293               | 24,208,517                 | 80.01                                | 3,152,686                  | 10.4                                 | 1,818,018                         | 5.99  |
|                                 |                     |                                    | Conventional | 0                | B0X/C10                   | 32,050,429               | -                          | -                                    | 30,671,378                 | 95.69                                | 22,184,190                        | 69.17 |
| <i>C. annuum</i> (Mock control) | -                   | -                                  | Conventional | 0                | B1X/C10                   | 30,610,179               | 27,162,689                 | 88.7                                 | -                          | -                                    | -                                 | -     |

<sup>a</sup> B1X, 1X volume of Dynabeads; B3.3X, 3.3X volume of Dynabeads and B0X, not addition of Dynabeads; C (10, 12, 15 and 20), number of PCR cycles in PCR enrichment step

<sup>b</sup> Trimmed reads with the mean of two or three replicates

<sup>c</sup> Number of reads (mean of two or three replicates) mapped to the plant or bacterial genome

<sup>d</sup> Percentage of mapped reads (average of two or three replicates)

<sup>e</sup> Number of reads (mean of two or three replicates) mapped to the bacterial coding sequences (CDS)

<sup>f</sup> Percentage of mapped reads to the bacterial CDS (average of two or three replicates)

bacteria, and subsequently facilitate transcriptome analysis, we have introduced modifications to two key steps within the strand-specific RNA sequencing (ssRNA-seq) library preparation protocol, as illustrated in Fig. 1. The initial step pertains to the removal of rRNA. In our efforts to boost the bacterial mRNA yield, we undertook a dual approach aimed at concomitantly eliminating rRNA. This involved employing both the mRNA enrichment method through the subtraction of plant poly (A) using Dynabeads and rRNA depletion for both bacterial and plant components. Following the removal of poly A and depletion of rRNA, the resultant samples were employed in the construction of RNA-seq libraries. To further enhance the enrichment of bacterial mRNA, a second modification was implemented during the PCR enrichment step within the ssRNA sequencing library preparation process (Fig. 1). By varying the number of PCR cycles, we systematically enriched the entire sample, including the bacterial mRNA. Consequently, we conducted experiments to assess and optimize the enrichment of bacterial mRNAs with different PCR cycle numbers and compared them with the typical PCR cycle number of 10. In our enriched method, we employed an increased concentration of

Dynabeads (3.3X) and subsequently assessed its impact in comparison to the standard 1X Dynabeads concentration, which is generally utilized for ssRNA-seq library preparation (Table 1). Overall, we assessed the effectiveness of two RNA-seq approaches: (i) the standard Illumina RNA-seq method (conventional method), which comprises of poly A removal using 1X concentration of Dynabeads, rRNA depletion using Ribozero, and a PCR enrichment step using a constant PCR cycle (10) (ii) the bacterial mRNA enrichment method (enriched method) which involves the subtraction of poly A using 3.3X Dynabeads, rRNA depletion using Ribozero, and a modified PCR enrichment step with varied number of PCR cycles (10, 12, 15, and 20). To effectively capture the distinct transcriptional responses of both bacteria and the host, it is crucial to carefully select time points that correspond to various stages of the infection process. During the initial stages of infection, it is probable that only a small amount of bacterial RNA is present, especially when employing low MOIs (Multiplicities of Infection). Therefore, in this investigation, we conducted transcript analysis of *F. dauae* inoculated tomato roots at 48 hpi, and for Xag8ra and Xcv3 infections in pepper plants,

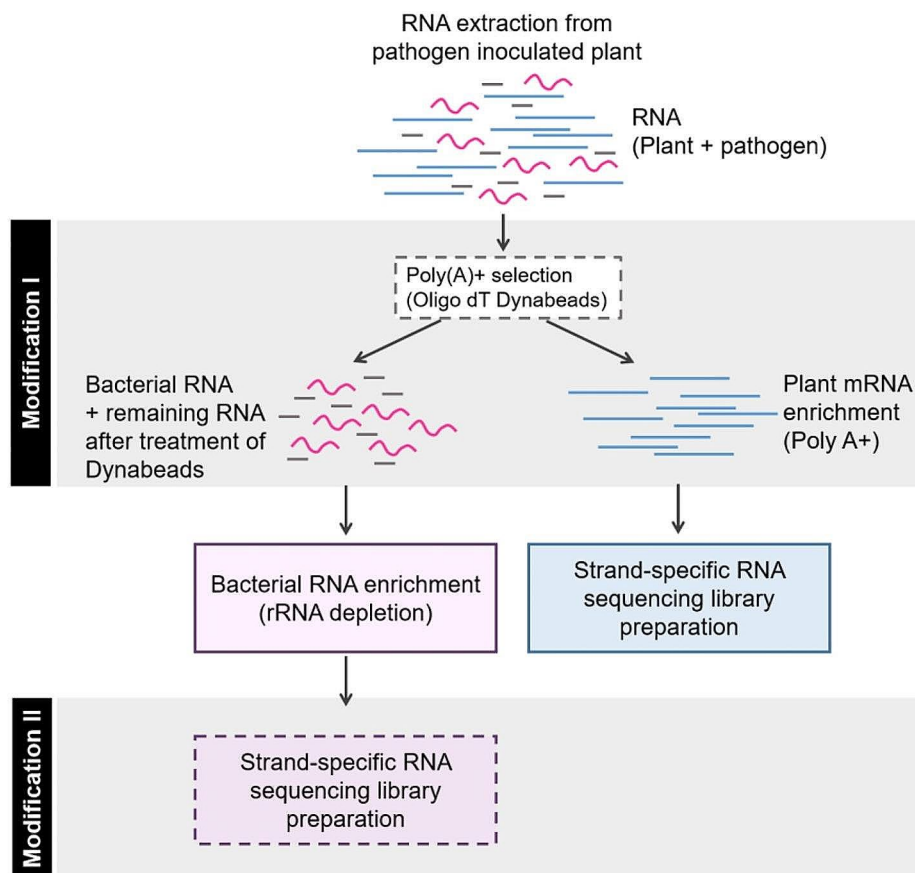


**Fig. 1** An overview of modified workflow for bacterial mRNA enrichment in dual RNA sequencing library preparation method

transcript analysis was performed at 12, 24, and 48 hpi employing both conventional and enriched methodologies (Table 1). Including appropriate mock-infected control samples for both the pathogen and the host is crucial for distinguishing between host responses that are specific or nonspecific to the bacterium. Hence, we used mock controls corresponding to the host (*C. annuum*) and the pathogen (*Xcv3*) in the current study.

#### **Effect of rRNA depletion on the mapping ratio to the genome and CDS of bacteria**

As the maximum depletion of rRNA and retrieval of mRNA reduces sequencing costs, we aimed to deplete rRNA (from both plant and bacteria) and retrieve mRNA through poly A selection simultaneously. A total of 44 RNA-seq libraries were generated including 16 libraries for the conventional method and 28 libraries for the enriched method. Subsequently, the raw RNA sequences were filtered and trimmed after sequencing. The processed reads from the conventional method generated an average of 119 M clean reads, while the enriched method produced approximately 18 M clean reads in *F. dauae* infected tomato samples (B3.3X/C10 in Table 1). Upon aligning the reads to the *F. dauae* genome and its coding sequences (CDS), the conventional method exhibited mapping rates of 1.2% and 0.15% to the genome and CDS respectively. Conversely, the enriched method displayed markedly higher mapping ratios, with 1.94% and 0.99% of reads aligning to the genome and CDS, respectively of *F. dauae*. This represents an increase of approximately 1.62-fold for genome mapping and 6.6-fold for CDS mapping of *F. dauae* compared to the conventional method (Table 1). In the context of *Xcv3*-infected pepper plants, the conventional method produced clean reads ranging from 30 M to 34 M reads at different time points while the enriched method yielded a wider range of reads, varying from 23 M to 45 M reads across various time points and different PCR cycle numbers. When compared to the conventional method, the enriched method exhibited a substantially higher mapping ratio of reads to the genome and CDS of *Xcv3*. Notably, at 48 hpi, the enriched method demonstrated a mapping ratio of 15.09% to the genome and 8.92% to the CDS of *Xcv3*. These values indicated a substantial improvement, with a 1.45-fold increase in genome mapping and a 1.49-fold increase in CDS mapping of *Xcv3* compared to the conventional method. Although the enriched method yielded a lower read count than the conventional method, it demonstrated an enhanced mapping ratio. The variation observed in the ratio of clean read count between *F. dauae*-infected tomato and *Xcv3*-infected pepper samples across the two methods could be attributed to variations in several factors including bacterial load, transcriptome complexity, host response variability,

specificity and efficacy of enrichment, as well as experimental and biological variability. Taken together, these results suggest that the modification involving simultaneous rRNA depletion and PCR enrichment in the enriched method leads to an elevated proportion of bacterial mRNA, at a reduced sequencing depth in plant-bacterial samples.

#### **Effect of modified PCR enrichment step on the mapping ratio and RNA-seq library preparation**

To enhance the abundance of bacterial mRNA in the sequencing reads, we adjusted the number of PCR cycles in the enriched method, as compared to the conventional ssRNA-seq library preparation method, which typically utilizes 10 PCR cycles with 5 µg of total RNA. The reads were aligned to bacterial genome and CDS in order to evaluate the increase in bacterial mRNA as the number of PCR cycle increases. Distinct responses were observed in the mapping ratios of *F. dauae* infected tomato as well as *Xcv3* and *Xag8ra* infected hot peppers in relation to variations in PCR cycle numbers. In case of *F. dauae* infected tomato, an inverse relationship was observed between the read mapping ratio and PCR cycles (Fig. 2A). However, in hot peppers infected with *Xcv3* and *Xag8ra*, a positive correlation where an increase in PCR cycle number is accompanied by a corresponding increase in the mapping ratio was observed (Table 1) (Fig. 2B, C). While an increase in PCR cycles improved the mapping ratio of *Xcv3* and *Xag8ra* infected pepper samples, it did not yield the desired library length, as evidenced by the size distribution pattern of cDNA libraries (Fig. S1). Therefore, the variations in mapping ratios at different PCR cycle numbers across different samples could be influenced by several factors that reflect the complex interplay between host-bacterial interactions, including host immune responses, bacterial virulence factors, infection dynamics and host specificity. Among all the examined libraries, the 10 and 12 PCR cycles exhibited a single peak corresponding to the expected library length, thus confirming the precise construction of these libraries. Conversely, the libraries subjected to 15 and 20 PCR cycles displayed either a collapsed peak or a secondary peak of unexpected size, indicating the generation of artifacts due to excessive PCR cycling (Fig. S1). Overall, the findings imply that despite the presence of a limited quantity of bacterial mRNA in 10 or 12 PCR cycles than higher PCR cycle numbers, it was appropriate for the ssRNA-seq library preparation with 5 µg of total RNA in the initial step.

#### **Mapping and gene expression profile of *Xcv3* infected pepper at various time points**

A hierarchical clustering was performed to identify the phylogenetic relationship between the mapping profiles

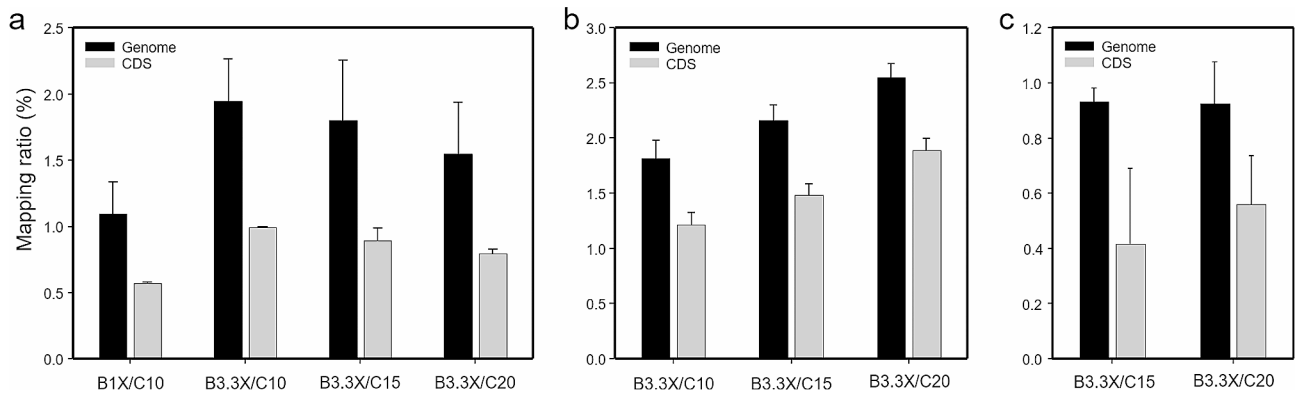


**Fig. 2** Impact of bacterial mRNA enrichment in Dual RNA-seq on genome and CDS mapping ratio. Ratio of reads aligned with (a) genome and CDS of *F. dauae* from *F. dauae* infected tomato at 48 hpi, (b) genome and CDS of *Xcv3* from *Xcv3* infected pepper at 24 hpi, and (c) genome and CDS of *Xag8ra* from *Xag8ra* inoculated pepper at 48 hpi. B, Dynabeads; 1X, 1X volume of Dynabeads as the original protocol; 3.3X, 3.3X volume of Dynabeads in the enriched protocol; C, number of PCR cycles in PCR enrichment step

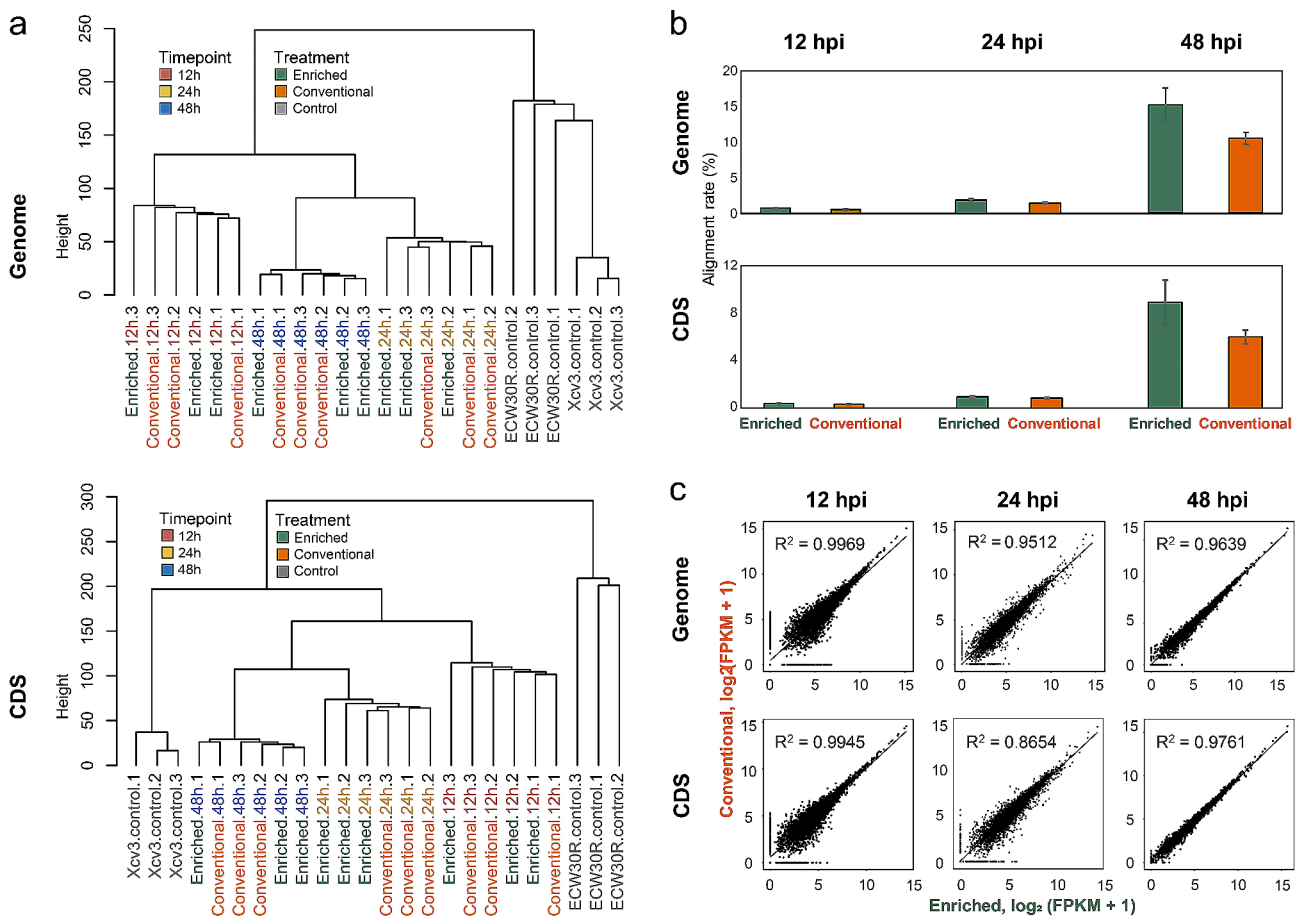


**Fig. 3** Mapping profiles to genome and CDS of conventional and enriched RNA-seq libraries using *Xcv3* transcripts. (a) Hierarchical clustering by mapping ratio to pathogen genome and CDS. (b) The average rate of aligned reads to reference genome and CDS for each library preparation method at same time points. All data indicate the average of mapping ratio  $\pm$  SD from three replicates of RNA-seq. (c) Pairwise comparison of mean normalized gene expression using all samples for each library preparation method.  $R^2$ , coefficient of determination value

of *Xcv3* infected pepper to the genome as well as to the CDS of *Xcv3* at various time points (Fig. 3A). The mapping patterns of samples from each time point to the genome of the pathogen were similar and they were

grouped together, regardless of the diverse sequencing methods employed. This suggests that the transcript profiles are distinct and characteristic of specific time points. A similar clustering pattern was also noticed when



examining the mapping profiles of reads to the CDS of the pathogen among different time points. The mock control samples (ECW30R and Xcv3) exhibited a similar mapping profile to their respective genomes and were grouped together in one cluster. However, their mapping patterns to the CDS differed noticeably, leading to the formation of distinct clusters (Fig. 3A).

The mapping profiles of reads from Xcv3 infected pepper samples to the genome and CDS of Xcv3 varied significantly among various time points (Fig. 3B). The mapping ratio to both the genome and CDS increased as the time of infection increased. The enriched method yielded the highest alignment rates (15.09% and 8.92%), when aligning the reads from samples collected at 48 hpi to the genomic and CDS of the pathogen, respectively. Further, a pairwise comparison of mean normalized gene expression was performed between the conventional and enriched method using all the biological replicates for each time point (Fig. 3C). When examining the gene expression values represented as the fragments per kilo base of transcript per million mapped reads (FPKM) at different time points, it became evident that there was a stronger correlation ( $R^2=0.99$ ) among the biological replicates from conventional and enriched methods at 12 and 24 hpi, irrespective of genome or CDS region. Relatively, a lower correlation ( $R^2=0.96$ ;  $R^2=0.97$ ) in terms of gene expression was observed when comparing samples between the conventional and enriched methods at 48 hpi for mapping to the genome and CDS respectively. Thus, the results indicated that peppers infected with Xcv3 exhibit significant dynamics in the mapping ratio and gene expression profile across various infection time points consistent to both conventional and enriched methods.

#### Differential gene expression analysis at various points of Xcv3 infection

The differential gene expression analysis in Xcv3 infected pepper plants showed significant differences in Differentially Expressed Genes (DEGs) between conventional and enriched methods at various infection time points. Differences in the number of DEGs were evaluated by comparing the conventional and enriched methods across various fold change (FC) thresholds represented as  $\log_2$  FC (Fig. 4). In both methods, there was a significant upregulation of genes associated with different infection time intervals. The number of genes that are upregulated and downregulated are indicated in Table S2. The enriched method consistently exhibited an elevated number of DEGs than the conventional method at all fold change threshold levels examined at various time points. Among all fold change threshold levels examined,  $\log_2$  FC > 0.5 showed the highest count of DEGs (294) in the enriched method than the conventional method (246)

during an early infection time (12 hpi). At the later stage of infection (48 hpi), a significantly reduced number of DEGs were observed in both the methods. However, a larger set of common genes (1,886) between the two methods was identified at 48 hpi at  $\log_2$  FC > 0.5. Overall, in the context of the enriched method, the examination of DEGs at different time points revealed that 24 hpi displayed the highest number of DEGs across all fold change threshold levels except  $\log_2$  FC > 0.5 (Fig. 4). Additionally, to verify this result, among DEG genes, six genes (CAJ23004, CAJ22057, CAJ22060, CAJ22069, CAJ24688, CAJ25348, CAJ21932) were randomly selected, and their expression was confirmed by qRT-PCR (Fig. S2A). In subsequent qRT-PCR analysis, these genes had similar expression patterns showing high induction compared with those in RNA-seq analysis (Fig. S2B).

#### Gene ontology enrichment analysis

An assessment of the biological functions of all the identified DEGs obtained through both conventional and enriched methods was done using Gene Ontology (GO) enrichment analysis. The bubble plot analysis revealed a significant enrichment of DEGs at various infection time points. Particularly, this enrichment was more pronounced at the 48 hpi using the enriched method (Fig. 5). When examining the top 20 DEGs among the enriched and conventional methods, it became evident that they displayed enrichment in similar GO terms, including various biological processes and molecular functions. In terms of biological processes, DEGs were significantly enriched in proteolysis and protein secretion by the type III secretion system. Thus, the secretion of proteolytic enzymes and translocation of effector proteins could aid the pathogen to invade and cause infection in the host plants. Within molecular function, significant enrichment of DEGs was observed in kinases, serine-type endopeptidases, and heme binding activities. This demonstrates that the enriched method has proven to be equally effective as the conventional method in elucidating gene ontology.

#### Discussion

The bacterial spot disease in tomato and pepper plants is attributed to the pathogen Xcv, while Xag is responsible for inducing HR in these plants [50, 51]. The necrotrophic pathogen Xag triggers the development of a bacterial pustule in its host plant, soybean, but does not elicit disease symptoms in non-host plant like hot pepper under natural conditions [30, 32]. Nonetheless, the infiltration of Xag into leaf tissues of non-host plants results in HR, which are associated with the activation of HR and pathogenicity genes (*hrp*) [52]. Reports indicate that the pathogen Xcv triggers cell death in pepper plants while inhibiting defense responses in tomato plants [30, 53].

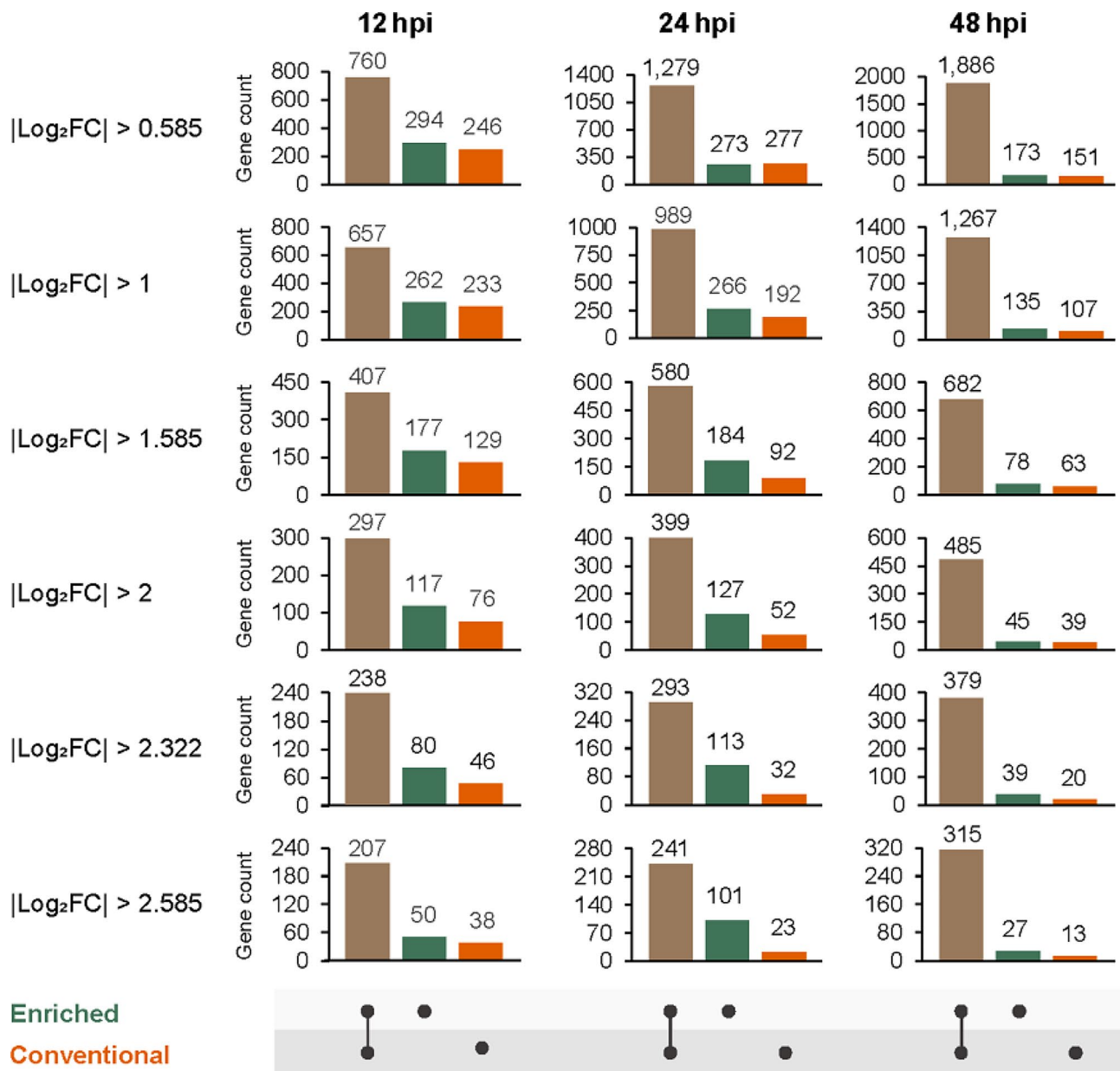


**Fig. 4** Number of differentially expressed genes (DEGs) in Xcv3 by enriched and conventional RNA-seq library preparation. Graphs in red, green and brown color indicate the number of DEGs identified in conventional, enriched and both methods respectively according to the series of log<sub>2</sub>FC

Simultaneous analysis of the gene expression of the two interacting species is valuable for gaining a thorough understanding of plant–bacterial interactions as it can reveal new virulence factors and host response pathways. RNA-seq allows for the simultaneous measurement of expression levels of numerous genes, offering valuable insights into functional pathways and regulatory networks involved in host–pathogen interactions [54, 55]. In the present study, we attempted to evaluate the efficiency of bacterial mRNA enrichment method in dual RNA sequencing involving three types of plant–bacterial interactions such as (i) incompatible host resistant response

in Xcv3 infected pepper, (ii) incompatible non–host resistant response in Xag infected pepper and (iii) positive/beneficial response in *F. dulae* infected tomato plants.

In order to facilitate effective transcript and gene detection, it is essential to eliminate highly abundant rRNAs from total RNA prior to sequencing. Common techniques involve the isolation of polyadenylated RNA (poly A) transcripts using oligo (dT) primers and the removal of excessively abundant rRNAs through hybridization capture, followed by separation using magnetic beads. The standard RNA sequencing approaches uses rRNA depletion alone or in combination with poly A selection

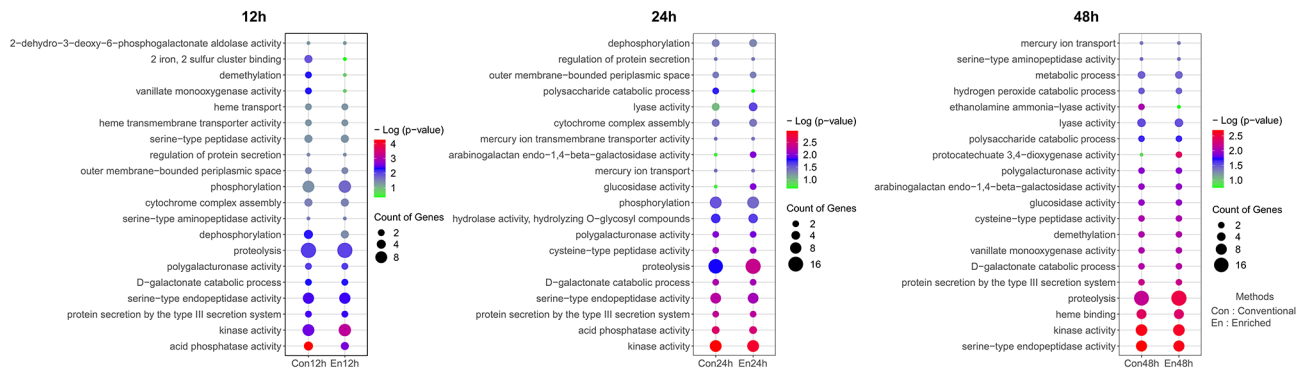


**Fig. 5** The Gene Ontology (GO) enrichment analysis of *C. annuum* infected by *Xcv3*. The bubble chart showing the enrichment of DEGs associated with various biological and molecular functions at various infection time points between the conventional and enriched methods. The bubble color indicates  $-\log(p\text{-value})$  and the bubble size indicates the gene count. The chart displays the top 20 GO terms. The y-axis indicates the GO terms, and the x-axis indicates the  $-\log(p\text{-value})$ . The term 'Con' indicates the conventional method while 'En' indicates the enriched method

depending upon the specific goal of the experiment [56, 57]. While the rRNA depletion approach captures both poly A+ and poly A- transcripts, the poly A+ selection method only captures transcripts with poly A tails. The results of a study by Zhao et al. [10] showed that just 6% of the reads from the poly A selection method were mapped to the intronic region, compared to about 50% of the reads from the rRNA depletion method. As a result, the poly A selection approach had substantially greater percentages of useable reads for gene quantification than the rRNA depletion method. However, numerous additional mRNAs without poly A tails are also excluded by poly A selection. The rRNA depletion strategy alone was able to identify new protein-coding genes, pseudogenes, short RNAs and lncRNAs (long non-coding RNAs) [10, 58]. For instance, the involvement of lncRNAs in the response of kiwifruit to *Pseudomonas syringae* pv. *actinidiae* infection has been revealed in a study [11]. Moreover, rRNA-depleted libraries are superior to poly A-selected libraries for degraded RNA samples [23, 59], and RNA-seq data from rRNA depletion offer novel insights into the transcriptional processes in cells [60]. Therefore, combining the two approaches (rRNA depletion and poly A selection) in dual RNA sequencing would be ideal to acquire deeper insights into the transcriptomic profiles of host-pathogen interactions because both selectively omit a diverse set of RNAs or target different fractions of the transcriptome. In this study, we have developed an effective dual RNA sequencing technique that uses both rRNA depletion and poly A selection to particularly enhance the bacterial mRNA in the mixed plant-bacterial samples. In comparison to the conventional method, the enriched method in our study using increased Dynabeads concentration (3.3X) has significantly improved the mapping ratio of *F. dauae* infected tomato, *Xcv3* and *Xag8ra* infected peppers to the genome and CDS of their respective bacteria (Table 1; Fig. 2). Consistent with our study, Kumar et al. [61] have demonstrated that the bacterial

mRNA enrichment method involving the concurrent removal of poly A and rRNA has tripled the amount of mRNA and the percentage of *Wolbachia* transcripts in a *Wolbachia-Drosophila* system.

While an increase in PCR cycles improved the mapping ratio of *Xcv3* and *Xag8ra* infected peppers, it did not produce the necessary library length, as revealed by the size distribution pattern of cDNA libraries (Fig. S1). Hence it was confirmed that 10/12 PCR cycles was optimum for the ssRNA-seq library preparation using the enriched method. Upon examining different infection time points of *Xcv3* in peppers, it was observed that the mapping ratio to the genome and CDS of *Xcv3* increased as the time of infection increases (Fig. 3B). This finding corresponds with the fact that the amount of bacterial RNA in the infected plant tissue increases as time elapses leading to an increased pathogen mapping ratio. Similar to our finding, Li et al. [62] also observed a higher mapping ratio during compatible and incompatible interactions between potato and *Phytophthora infestans* at the later stage of infection (48 hpi). However, a significant correlation existed among the conventional and enriched methods in terms of gene expression during early stages of infection in 12 and 24 hpi (Fig. 3C). Consistent to this result, the number of DEGs were found greatly upregulated in early infection time points (Fig. 4). A significant upregulation of DEGs was obtained in the enrichment method at all examined fold change thresholds than that of the conventional method. The number of DEGs were maximum at 24 hpi in the enriched method irrespective of all fold change thresholds. The number of DEGs notably reduced at the later stage of infection (48 hpi) at both RNA-seq methods. This suggests that the host plant has displayed an effective defense response against the bacterial pathogen, *Xcv3* during later stages of infection. Similar to our study, the number of upregulated DEGs were greatly reduced at the late stage of infection (60 hpi) by *Phytophthora nicotianae* in susceptible tobacco cultivar

(XHJ) [63]. Likewise, in a *Brassica napus* line susceptible to stem rot causing fungal pathogen, *Sclerotinia sclerotiorum*, there were fewer number of differentially expressed genes at the late infection stages (24–48 hpi) compared to the early infection stages (8–16 hpi) [64]. Hence, our study employing the enriched method, proved to be effective in detecting a greater number of DEGs in the initial phases of infection, when bacterial RNA levels are relatively lower in comparison to the later stages of infection.

The GO analysis showed that, in both conventional and enriched approaches, particularly at 48 hpi, a considerable enrichment of DEGs occurred in activities linked to proteolysis, protein secretion by the type III secretion system (T3SS), kinases, serine-type endopeptidases, and heme binding (Fig. 5). Proteolysis serves multiple critical functions throughout the entire infection cycle of the pathogen, contributing significantly to its virulence mechanisms. Secreted proteases play a crucial role in promoting host penetration and effective dissemination by actively engaging in breaking down the host's physical defenses [65]. Furthermore, proteolytic enzymes facilitate host colonization by counteracting the host's defense mechanisms [66].

The T3SS is a common strategy used by many gram-negative bacteria to invade plants, including *Xanthomonas campestris* pv. *vesicatoria*. This system includes a translocon, a bacterial protein channel that integrates into the plasma membrane of the host and aids in the translocation of effector proteins into the host cell cytosol [67, 68]. The type III effectors are thought to impair a variety of host cellular processes, including cytoskeletal adjustments, vesicle transport, and defense reactions [69, 70]. The T3SS is encoded by a gene cluster known as *hrp* which are responsible for inflicting disease on susceptible plants while inducing the hypersensitive response, a rapid programmed cell death occurring at the site of infection on resistant plants [71, 72]. The genes involved in T3SS that encode *HrpA*, *HrpB*, *HrpD* etc. exhibited elevated expression levels during *Pantoea stewartii* subsp. *stewartii* infection in corn plants leading to Stewart's wilt disease [73]. Prior research using a luminous reporter demonstrated the active transcription of *hrp* genes encoding T3SS and its effectors during the late stages of infection with *Ralstonia solanacearum*, the causative agent of bacterial wilt in species of solanaceous plants [74]. Recently, a comprehensive investigation of *in planta* transcriptome of *R. solanacearum*, has demonstrated a significant upregulation of *hrp* genes and T3SS effectors in the xylem of asymptomatic/wilted potato plants [75].

Kinases are central players in the intricate signaling pathways involved in bacterial infections. They are involved in regulating both host responses to infection

and bacterial virulence strategies. The hallmark of signaling pathways is the process of serine/threonine phosphorylation by kinases, followed by dephosphorylation by phosphatases [76]. In a previous study, the two component signaling pathway elements such as histidine kinases (HKs) and response regulators (RR) that regulate a mitogen-activated protein kinase cascade were found to be upregulated during the infection of *Fusarium oxysporum* causing vascular wilt disease in banana [77]. Many studies have documented that pathogens also modulate certain serine threonine protein kinases in host plants during infection. For instance  $\text{Ca}^{2+}$  dependent protein kinases (CDPKs) were actively upregulated in fungal induced defense responses in potato [78], hybrid poplar [79], and *B. napus* [80]. Serine proteases are endopeptidases which are involved in several key functions including cell signaling, protein metabolism, protein processing, blood coagulation and immunity regulation [81, 82]. Additionally, they are apparently found as a virulence factor in a variety of pathogenic bacteria. For instance, the primary virulence factor of the phytopathogenic bacterium *Clavibacter michiganensis*, which causes tomato wilting and canker, is a putative serine protease encoded by the *pat-1* gene [83]. In Gram-negative bacteria, iron plays a vital role in growth and colonization in host, as it acts as a coenzyme in fundamental cellular processes like cellular respiration and DNA synthesis [84]. During infection, the host immune response employs a strategy known as nutritional immunity to restrict the availability of free iron to the pathogens [85]. Although hosts have developed strategies to sequester iron to impede bacterial growth, pathogenic bacteria have simultaneously evolved mechanisms to evade these host defenses. Notably, Gram-negative pathogens possess outer membrane receptors designed to acquire ferrous iron and release siderophores and hemophores to capture iron-containing compounds such as heme or hemoglobin, facilitating their uptake into the bacterial cells [86, 87]. The enrichment of DEGs associated with heme binding activity in our study implies the significance of iron acquisition during the infection process of the pathogen. Therefore, the findings of our investigation strongly indicate that, proteolysis, secretion of effector proteins through T3SS, kinases, serine type endopeptidase and heme binding activities play a central role in the infection process of Xcv3 in peppers.

## Conclusions

The present study has demonstrated an efficient bacterial mRNA enrichment method for the dual RNA-seq involving the concomitant rRNA removal and poly A selection with increased Dynabeads concentration. In comparison to the conventional RNA-seq method, a significant improvement in the alignment of reads to the

genomic as well as to the coding sequences of the pathogen was observed in the enriched method. At all fold change threshold levels studied at various stages of Xcv3 infection in peppers, the enriched method consistently showed a higher number of DEGs than the conventional method. Moreover, the enriched method was consistent with the conventional method in elucidating the GO terms with DEGs predominantly enriched in proteolysis, kinase, serine type endopeptidase and heme binding activities. Thus, the enriched method described in this study presents a novel and reliable approach to enhance the read mapping of bacterial counterparts in dual RNA-seq and decipher the complex transcriptomic changes involved in plant-bacterial interactions.

### Supplementary Information

The online version contains supplementary material available at <https://doi.org/10.1186/s13007-024-01227-x>.

Supplementary Material 1

### Author contributions

W-HK conceived and designed the study, JS wrote the original manuscript, H-AL, J-SK, JYN and HJ carried out experiments and collected the data, JL and J-SK analyzed and validated the data, JS interpreted the data, JS, JL and J-SK revised the manuscript, H-AL and W-HK critically reviewed the revised manuscript. All authors have reviewed and agreed to the final version of the manuscript.

### Funding

This work was supported by grants from the National Research Foundation of Korea (NRF) from the Korean government (NRF-2019R1C1C1007472 and RS-2024-00338092).

### Data availability

The datasets supporting the conclusions of this article are included within the article or are available from corresponding author on reasonable request.

### Declarations

#### Ethics approval and consent to participate

Not applicable.

#### Consent for publication

All authors agree with the submission of this manuscript to *Plant Methods*.

#### Competing interests

The authors declare no competing interests.

#### Author details

<sup>1</sup>Department of Horticulture, Division of Applied Life Science (BK21 Four Program), Institute of Agriculture & Life Science, Gyeongsang National University, Jinju 52828, Republic of Korea

<sup>2</sup>Division of Smart Horticulture, Yonam College, Cheonan 31005, Republic of Korea

Received: 11 January 2024 / Accepted: 22 June 2024

Published online: 01 July 2024

### References

1. Kwon JS, Shilpha J, Lee J, Yeom SI. Beyond NGS data sharing for plant ecological resilience and improvement of agronomic traits. *Sci Data*. 2024;11(1):466.

2. Rao MS, Van Vleet TR, Ciurlionis R, Buck WR, Mittelstadt SW, Blomme EAG, Liguori MJ. Comparison of RNA-Seq and microarray gene expression platforms for the Toxicogenomic evaluation of liver from short-term rat toxicity studies. *Front Genet*. 2018;9:636.
3. Zhao S, Fung-Leung WP, Bittner A, Ngo K, Liu X. Comparison of RNA-Seq and microarray in transcriptome profiling of activated T cells. *PLoS ONE*. 2014;9(1):e78644.
4. Hakim S, Imran A, Hussain MS, Mirza MS. RNA-Seq analysis of mung bean (*Vigna radiata* L.) roots shows differential gene expression and predicts regulatory pathways responding to taxonomically different rhizobia. *Microbiol Res*. 2023;275:127451.
5. Kang WH, Sim YM, Koo N, Nam JY, Lee J, Kim N, Jang H, Kim YM, Yeom SI. Transcriptome profiling of abiotic responses to heat, cold, salt, and osmotic stress of *Capsicum annuum* L. *Sci Data*. 2020;7(1):17.
6. Lee J, Yeom SI. Global co-expression network for key factor selection on environmental stress RNA-seq dataset in *Capsicum annuum*. *Sci Data*. 2023;10(1):692.
7. Sudhakar P, Andrighetti T, Verstockt S, Caenepeel C, Ferrante M, Sabino J, Verstockt B, Vermeire S. Integrated analysis of microbe-host interactions in Crohn's disease reveals potential mechanisms of microbial proteins on host gene expression. *iScience*. 2022;25(5):103963.
8. Yin L, Shen X, Yin D, Hou H, Wang J, Zhao R, Dai Y, Pan X, Qi K. Integrated analysis of noncoding RNAs and mRNAs reveals their potential roles in chicken spleen response to *Klebsiella variicola* infection. *Res Vet Sci*. 2023;164:105029.
9. Nuss AM, Beckstette M, Pimenova M, Schmuhl C, Opitz W, Pisano F, Heroven AK, Dersch P. Tissue dual RNA-seq allows fast discovery of infection-specific functions and riboregulators shaping host-pathogen transcriptomes. *Proc Natl Acad Sci U S A*. 2017;114(5):E791–800.
10. Zhao S, Zhang Y, Gamini R, Zhang B, von Schack D. Evaluation of two main RNA-seq approaches for gene quantification in clinical RNA sequencing: polyA + selection versus rRNA depletion. *Sci Rep*. 2018;8(1):4781.
11. Colgan AM, Cameron AD, Kroger C. If it transcribes, we can sequence it: mining the complexities of host-pathogen-environment interactions using RNA-seq. *Curr Opin Microbiol*. 2017;36:37–46.
12. Ma SH, He GQ, Navarro-Paya D, Santiago A, Cheng YZ, Jiao JB, Li HJ, Zuo DD, Sun HT, Pei MS, et al. Global analysis of alternative splicing events based on long- and short-read RNA sequencing during grape berry development. *Gene*. 2023;852:147056.
13. Wang Z, Liu Y, Li L, Li D, Zhang Q, Guo Y, Wang S, Zhong C, Huang H. Whole transcriptome sequencing of *Pseudomonas syringae* Pv. Actinidiae-infected kiwifruit plants reveals species-specific interaction between long non-coding RNA and coding genes. *Sci Rep*. 2017;7(1):4910.
14. Kim N, Lee J, Yeom SI, Kang NJ, Kang WH. The landscape of abiotic and biotic stress-responsive splice variants with deep RNA-seq datasets in hot pepper. *Sci Data*. 2024;11(1):381.
15. Westermann AJ, Gorski SA, Vogel J. Dual RNA-seq of pathogen and host. *Nat Rev Microbiol*. 2012;10(9):618–30.
16. Giannoukos G, Ciulla DM, Huang K, Haas BJ, Izard J, Levin JZ, Livny J, Earl AM, Gevers D, Ward DV, et al. Efficient and robust RNA-seq process for cultured bacteria and complex community transcriptomes. *Genome Biol*. 2012;13(3):R23.
17. Pang X, Zhou D, Song Y, Pei D, Wang J, Guo Z, Yang R. Bacterial mRNA purification by magnetic capture-hybridization method. *Microbiol Immunol*. 2004;48(2):91–6.
18. Yi H, Cho YJ, Won S, Lee JE, Jin Yu H, Kim S, Schroth GP, Luo S, Chun J. Duplex-specific nuclease efficiently removes rRNA for prokaryotic RNA-seq. *Nucleic Acids Res*. 2011;39(20):e140.
19. Armour CD, Castle JC, Chen R, Babak T, Loerch P, Jackson S, Shah JK, Dey J, Rohl CA, Johnson JM, et al. Digital transcriptome profiling using selective hexamer priming for cDNA synthesis. *Nat Methods*. 2009;6(9):647–9.
20. Peano C, Pietrelli A, Consolandi C, Rossi E, Petiti L, Tagliabue L, De Bellis G, Landini P. An efficient rRNA removal method for RNA sequencing in GC-rich bacteria. *Microb Inf Exp*. 2013;3(1):1.
21. Wahl A, Huptas C, Neuhaus K. Comparison of rRNA depletion methods for efficient bacterial mRNA sequencing. *Sci Rep*. 2022;12(1):5765.
22. He S, Wurtzel O, Singh K, Froula JL, Yilmaz S, Tringe SG, Wang Z, Chen F, Lindquist EA, Sorek R, et al. Validation of two ribosomal RNA removal methods for microbial metatranscriptomics. *Nat Methods*. 2010;7(10):807–12.
23. Kamminga T, Benis N, Martins Dos Santos V, Bijlsma JJE, Schaap PJ. Combined transcriptome sequencing of *Mycoplasma hyopneumoniae* and infected Pig Lung tissue reveals Up-Regulation of bacterial F1-Like ATPase and down-regulation of the P102 cilium adhesin in vivo. *Front Microbiol*. 2020;11:1679.

24. Robbe-Saule M, Babonneau J, Sismeiro O, Marsollier L, Marion E. An optimized method for extracting bacterial RNA from mouse skin tissue colonized by *Mycobacterium ulcerans*. *Front Microbiol.* 2017;8:512.
25. Ciulla D, Giannoukos G, Earl A, Feldgarden M, Gevers D, Levin J, Livny J, Ward D, Gnirke A, Nusbbaum C. Evaluation of bacterial ribosomal RNA (rRNA) depletion methods for sequencing microbial community transcriptomes. *Genome Biol.* 2010;11:1–1.
26. Petrova OE, Garcia-Alcalde F, Zampaloni C, Sauer K. Comparative evaluation of rRNA depletion procedures for the improved analysis of bacterial biofilm and mixed pathogen culture transcriptomes. *Sci Rep.* 2017;7(1):41114.
27. Herbert ZT, Kershner JP, Butty VL, Thimmapuram J, Choudhari S, Alekseyev YO, Fan J, Podnar JW, Wilcox E, Gipson J, et al. Cross-site comparison of ribosomal depletion kits for illumina RNAseq library construction. *BMC Genomics.* 2018;19(1):199.
28. Nobori T, Velasquez AC, Wu J, Kvitko BH, Kremer JM, Wang Y, He SY, Tsuda K. Transcriptome landscape of a bacterial pathogen under plant immunity. *Proc Natl Acad Sci U S A.* 2018;115(13):E3055–64.
29. Ramskold D, Luo S, Wang YC, Li R, Deng Q, Faridani OR, Daniels GA, Khrebtkova I, Loring JF, Laurent LC, et al. Full-length mRNA-Seq from single-cell levels of RNA and individual circulating tumor cells. *Nat Biotechnol.* 2012;30(8):777–82.
30. Sorek R, Cossart P. Prokaryotic transcriptomics: a new view on regulation, physiology and pathogenicity. *Nat Rev Genet.* 2010;11(1):9–16.
31. Yeom SI, Seo E, Oh SK, Kim KW, Choi D. A common plant cell-wall protein HyPRP1 has dual roles as a positive regulator of cell death and a negative regulator of basal defense against pathogens. *Plant J.* 2012;69(5):755–68.
32. Utami D, Meale SJ, Young AJ. A pan-global study of bacterial leaf spot of chili caused by *Xanthomonas* spp. *Plants (Basel).* 2022;11(17):2291.
33. Glick BR. Plant growth-promoting bacteria: mechanisms and applications. *Scientifica (Cairo).* 2012;2012:963401.
34. Jung EJ, Choi SY, Lee SM, Song JY, Lee HJ, Kim E, et al. *Flavobacterium dauae* sp. nov., isolated from rhizosphere soil of a tomato plant. *Int J Syst Evol Microbiol.* 2021;71(10):004604.
35. Kang WH, Lee J, Koo N, Kwon JS, Park B, Kim YM, Yeom SI. Universal gene co-expression network reveals receptor-like protein genes involved in broad-spectrum resistance in pepper (*Capsicum annuum* L.). *Hortic Res.* 2022;9.
36. Levin JZ, Yassour M, Adiconis X, Nusbbaum C, Thompson DA, Friedman N, Gnirke A, Regev A. Comprehensive comparative analysis of strand-specific RNA sequencing methods. *Nat Methods.* 2010;7(9):709–15.
37. Kim MS, Kim S, Jeon J, Kim KT, Lee HA, Lee HY, Park J, Seo E, Kim SB, Yeom SI, et al. Global gene expression profiling for fruit organs and pathogen infections in the pepper, *Capsicum annuum* L. *Sci Data.* 2018;5:180103.
38. Lee J, Nam JY, Jang H, Kim N, Kim YM, Kang WH, Yeom SI. Comprehensive transcriptome resource for response to phytohormone-induced signaling in *Capsicum annuum* L. *BMC Res Notes.* 2020;13(1):440.
39. Martin M. Cutadapt removes adapter sequences from high-throughput sequencing reads. *EMBnet J.* 2011;17(1):10–2.
40. Bolger AM, Lohse M, Usadel B. Trimmomatic: a flexible trimmer for illumina sequence data. *Bioinformatics.* 2014;30(15):2114–20.
41. Kopylova E, Noe L, Touzet H. SortMeRNA: fast and accurate filtering of ribosomal RNAs in metatranscriptomic data. *Bioinformatics.* 2012;28(24):3211–7.
42. Quast C, Priesse E, Yilmaz P, Gerken J, Schweer T, Yarza P, Peplies J, Glockner FO. The SILVA ribosomal RNA gene database project: improved data processing and web-based tools. *Nucleic Acids Res.* 2013;41(Database issue):D590–596.
43. Kim D, Langmead B, Salzberg SL. HISAT: a fast spliced aligner with low memory requirements. *Nat Methods.* 2015;12(4):357–60.
44. Lee JS, Jang HK, Kang WH, Yeom SI. Transcriptome analysis of pepper-*Phytophthora infestans* interaction based on a pipeline of a simplified and effective RNA-seq analysis (PoRAS). *Hortic Sci Technol.* 2023;41(1):100–110.
45. Love MI, Huber W, Anders S. Moderated estimation of fold change and dispersion for RNA-seq data with DESeq2. *Genome Biol.* 2014;15(12):550.
46. Gotz S, Garcia-Gomez JM, Terol J, Williams TD, Nagaraj SH, Nueda MJ, Robles M, Talon M, Dopazo J, Conesa A. High-throughput functional annotation and data mining with the Blast2GO suite. *Nucleic Acids Res.* 2008;36(10):3420–35.
47. Young MD, Wakefield MJ, Smyth GK, Oshlack A. Goseq: gene ontology testing for RNA-seq datasets. *R Bioconductor.* 2012;8:1–25.
48. H W. ggplot2. *Wiley Interdiscip Rev Comput Stat.* 2011;3:180–5.
49. Almeida NF, Yan S, Cai R, Clarke CR, Morris CE, Schaad NW, Schuenzel EL, Lacy GH, Sun X, Jones JB. PAMDB, a multilocus sequence typing and analysis database and website for plant-associated microbes. *Phytopathology.* 2010;100(3):208–15.
50. Kaewnum S, Prathuangwong S, Burr T. Aggressiveness of *Xanthomonas axonopodis* Pv. *Glycines* isolates to soybean and hypersensitivity responses by other plants. *Plant Pathol.* 2005;54(3):409–15.
51. Potnis N, Timilsina S, Strayer A, Shantharaj D, Barak JD, Paret ML, Vallad GE, Jones JB. Bacterial spot of tomato and pepper: diverse *Xanthomonas* species with a wide variety of virulence factors posing a worldwide challenge. *Mol Plant Pathol.* 2015;16(9):907–20.
52. Chang SP, Jeon YH, Kim YH. Defense-related responses in fruit of the nonhost chili pepper against *Xanthomonas axonopodis* Pv. *Glycines* infection. *Plant Pathol J.* 2016;32(4):311–20.
53. Kim NH, Choi HW, Hwang BK. *Xanthomonas campestris* Pv. *Vesicatoria* effector AvrBsT induces cell death in pepper, but suppresses defense responses in tomato. *Mol Plant Microbe Interact.* 2010;23(8):1069–82.
54. Saliba AE, Vogel SCS. New RNA-seq approaches for the study of bacterial pathogens. *Curr Opin Microbiol.* 2017;35:78–87.
55. Westermann AJ, Barquist L, Vogel J. Resolving host-pathogen interactions by dual RNA-seq. *PLoS Pathog.* 2017;13(2):e1006033.
56. Conesa A, Madrigal P, Tarazona S, Gomez-Cabrero D, Cervera A, McPherson A, et al. A survey of best practices for RNA-seq data analysis. *Genome Biol.* 2016;17:1–19.
57. Hrdlickova R, Toloue M, Tian B. RNA-Seq methods for transcriptome analysis. *Wiley Interdiscip Rev RNA.* 2017;8(1):e1364.
58. Guo Y, Zhao S, Sheng Q, Guo M, Lehmann B, Pietenpol J, Samuels DC, Shyr Y. RNAseq by total RNA library identifies additional RNAs compared to poly(A) RNA library. *Biomed Res Int.* 2015;2015:862130.
59. Schuierer S, Carbone W, Knehr J, Petitjean V, Fernandez A, Sultan M, Roma G. A comprehensive assessment of RNA-seq protocols for degraded and low-quantity samples. *BMC Genomics.* 2017;18(1):442.
60. Gaidatzis D, Burger L, Florescu M, Stadler MB. Analysis of intronic and exonic reads in RNA-seq data characterizes transcriptional and post-transcriptional regulation. *Nat Biotechnol.* 2015;33(7):722–9.
61. Kumar N, Lin M, Zhao X, Ott S, Santana-Cruz I, Daugherty S, Rikihisa Y, Sadzewicz L, Tallon LJ, Fraser CM, et al. Efficient enrichment of bacterial mRNA from host-bacteria total RNA samples. *Sci Rep.* 2016;6:34850.
62. Li H, Hu R, Fan Z, Chen Q, Jiang Y, Huang W, Tao X. Dual RNA sequencing reveals the genome-wide expression profiles during the compatible and incompatible interactions between *Solanum tuberosum* and *Phytophthora infestans*. *Front Plant Sci.* 2022;13:817199.
63. Meng H, Sun M, Jiang Z, Liu Y, Sun Y, Liu D, Jiang C, Ren M, Yuan G, Yu W, et al. Comparative transcriptome analysis reveals resistant and susceptible genes in tobacco cultivars in response to infection by *Phytophthora nicotianae*. *Sci Rep.* 2021;11(1):809.
64. Chittem K, Yajima WR, Goswami RS, Del Rio Mendoza LE. Transcriptome analysis of the plant pathogen *Sclerotinia sclerotiorum* interaction with resistant and susceptible canola (*Brassica napus*) lines. *PLoS ONE.* 2020;15(3):e0229844.
65. Figaj D, Ambrozziak P, Przepiora T, Skorko-Glonek J. The role of proteases in the virulence of plant pathogenic bacteria. *Int J Mol Sci.* 2019;20(3):672.
66. Hueck CJ. Type III protein secretion systems in bacterial pathogens of animals and plants. *Microbiol Mol Biol Rev.* 1998;62(2):379–433.
67. Buttner D, Lorenz C, Weber E, Bonas U. Targeting of two effector protein classes to the type III secretion system by a HpaC- and HpaB-dependent protein complex from *Xanthomonas campestris* Pv. *Vesicatoria*. *Mol Microbiol.* 2006;59(2):513–27.
68. He SY, Nomura K, Whittam TS. Type III protein secretion mechanism in mammalian and plant pathogens. *Biochim Biophys Acta.* 2004;1694(1–3):181–206.
69. Espinosa A, Alfano JR. Disabling surveillance: bacterial type III secretion system effectors that suppress innate immunity. *Cell Microbiol.* 2004;6(11):1027–40.
70. Mudgett MB. New insights to the function of phytopathogenic bacterial type III effectors in plants. *Annu Rev Plant Biol.* 2005;56:509–31.
71. Bonas U, Schulte R, Fenselau S, Minsavage GV, Staskawicz BJ, Stall RE. Isolation of a gene cluster from *Xanthomonas campestris* Pv. *Vesicatoria* that determines pathogenicity and the hypersensitive response on pepper and tomato. *Mol Plant Microbe Interact.* 1991;4(1):81–8.
72. Weber E, Berger C, Bonas U, Koebnik R. Refinement of the *Xanthomonas campestris* Pv. *Vesicatoria* hrpD and hrpE operon structure. *Mol Plant Microbe Interact.* 2007;20(5):559–67.
73. Packard H, Kernell Burke A, Jensen RV, Stevens AM. Analysis of the in planta transcriptome expressed by the corn pathogen *Pantoea stewartii* subsp. *stewartii* via RNA-Seq. *PeerJ.* 2017;5:e3237.

74. Monteiro F, Genin S, van Dijk I, Valls M. A luminescent reporter evidences active expression of *Ralstonia solanacearum* type III secretion system genes throughout plant infection. *Microbiol.* 2012;158(8):2107–16.
75. de Pedro-Jove R, Puigvert M, Sebastia P, Macho AP, Monteiro JS, Coll NS, Setubal JC, Valls M. Dynamic expression of *Ralstonia solanacearum* virulence factors and metabolism-controlling genes during plant infection. *BMC Genomics.* 2021;22(1):170.
76. Jin J, Pawson T. Modular evolution of phosphorylation-based signalling systems. *Philos Trans R Soc Lond B Biol Sci.* 2012;367(1602):2540–55.
77. Guo L, Han L, Yang L, Zeng H, Fan D, Zhu Y, Feng Y, Wang G, Peng C, Jiang X, et al. Genome and transcriptome analysis of the fungal pathogen *Fusarium oxysporum* f. sp. *cubense* causing banana vascular wilt disease. *PLoS ONE.* 2014;9(4):e95543.
78. Blanco F, Zanetti M, Daleo GR. Calcium-dependent protein kinases are involved in potato signal transduction in response to elicitors from the Oomycete *Phytophthora infestans*. *J Phytopathol.* 2008;156(1):53–61.
79. Azaiez A, Boyle B, Levee V, Seguin A. Transcriptome profiling in hybrid poplar following interactions with *Melampsora rust* fungi. *Mol Plant Microbe Interact.* 2009;22(2):190–200.
80. Joshi RK, Megha S, Rahman MH, Basu U, Kav NN. A global study of transcriptome dynamics in canola (*Brassica napus* L.) responsive to *Sclerotinia sclerotiorum* infection using RNA-Seq. *Gene.* 2016;590(1):57–67.
81. Ekici OD, Paetzel M, Dalbey RE. Unconventional serine proteases: variations on the catalytic Ser/His/Asp triad configuration. *Protein Sci.* 2008;17(12):2023–37.
82. Patel S. A critical review on serine protease: key immune manipulator and pathology mediator. *Allergol Immunopathol (Madr).* 2017;45(6):579–91.
83. Hwang IS, Oh EJ, Song E, Park IW, Lee Y, Sohn KH, et al. An apoplastic effector Pat-1Cm of the gram-positive bacterium *Clavibacter michiganensis* acts as both a pathogenicity factor and an immunity elicitor in plants. *Front Plant Sci.* 2022;13:888290.
84. Sheldon JR, Laakso HA, Heinrichs DE. Iron acquisition strategies of bacterial pathogens. *Microbiol Spectr.* 2016;4(2):43–85.
85. Barber MF, Elde NC. Escape from bacterial iron piracy through rapid evolution of transferrin. *Science.* 2014;346(6215):1362–6.
86. Ellermann M, Arthur JC. Siderophore-mediated iron acquisition and modulation of host-bacterial interactions. *Free Radic Biol Med.* 2017;105:68–78.
87. Richard KL, Kelley BR, Johnson JG. Heme uptake and utilization by gram-negative bacterial pathogens. *Front Cell Infect Microbiol.* 2019;9:81.

### Publisher's Note

Springer Nature remains neutral with regard to jurisdictional claims in published maps and institutional affiliations.